

Theory of Solid He³†

N. BERNARDES

Institute for Atomic Research and Department of Physics, Iowa State University, Ames, Iowa

AND

H. PRIMAKOFF

Department of Physics, Washington University, St. Louis, Missouri

(Received March 30, 1960)

A theoretical analysis is given of the properties of solid He³ on the basis of: (1) a gas-phase Lennard-Jones "12-6" potential modified at small interatomic distances; (2) a Heitler-London type variational-trial wave function for all the atoms in the solid constructed from a properly antisymmetrized product of individual atom orbitals localized on the various lattice points; (3) a Dirac vector model to describe the symmetry energy with an exchange integral deduced from (1) and (2); (4) a spin-wave approximation at "low" temperatures and a Kramers-Opechowski approximation at "high" temperatures for calculation of the free energy of the nuclear spins; and (5) a Debye phonon model for the description of the vibrationally excited states of the solid. On this basis, calculated values at low pressures and temperatures ($p \approx 30$ atm; $T \lesssim 1$ °K) are presented for: (a) the cohesive energy

per atom; (b) the root mean square deviation of an atom from its lattice site: $\approx 0.36 \times$ nearest neighbor distance; (c) the nuclear magnetic susceptibility which corresponds to an antiferromagnetic behavior with a "paramagnetic" Curie temperature $T_C \approx 0.1$ °K; (d) the variation (decrease) of T_C with increasing pressure corresponding to a possible nuclear antiferromagnetic to nuclear ferromagnetic transition for $p \approx 150$ atm; (e) the specific heat which exhibits an anomaly at $T \approx 0.1$ °K associated with the alignment of the nuclear spins; (f) the thermal expansion coefficient which becomes negative below about 0.6 °K; (g) the melting curve which is characterized by a minimum at $T \approx 0.37$ °K and a maximum at $T \approx 0.08$ °K. Comparison of the theory is made with available experimental data.

1. INTRODUCTION

RELATIVELY little is known from experiment, at the moment of writing, about the properties of solid He³. Also, except for a few more or less qualitative discussions¹⁻³ with partially conflicting conclusions, no detailed quantitative treatment of the solid He³ problem has as yet been presented.

In the present paper we describe a theoretical analysis of the properties of solid He³ on the basis of: (1) a gas-phase Lennard-Jones "12-6" potential modified at small interatomic distances; (2) a Heitler-London type variational-trial wave function for all the atoms in the solid constructed from a properly antisymmetrized product of individual atom orbitals localized on the various lattice points; (3) a Dirac vector model to describe the symmetry energy with an exchange integral deduced from (1) and (2); (4) a spin-wave approximation at "low" temperatures, and a Kramers-Opechowski approximation at "high" temperatures, for calculation of the free energy of the nuclear spins, and (5) a Debye phonon model for the description of the vibrationally excited states of the solid. On this basis we calculate several properties of solid He³: cohesive energy, entropy, specific heat, coefficient of thermal expansion, nuclear magnetic susceptibility, etc., at pressures $p \approx 30$ atm and temperatures $T \lesssim 1$ °K as well as obtain the melting curve for $T < 0.5$ °K.⁴ A summary of the results may be

found in Sec. 10. The present paper supercedes the brief and preliminary account which has previously appeared.⁵

2. SPIN ALIGNMENT AND NUCLEAR MAGNETIC SUSCEPTIBILITY OF SOLID He³

Due to the relatively large zero point energy and weak interatomic attraction, a pressure of the order of 30 atm is necessary in order to solidify He³ (or He⁴) at temperatures $T \lesssim 1$ °K. As regards the He³ magnetic properties, Fairbank and his co-workers⁶ have measured the nuclear magnetic susceptibility of liquid He³ for a wide range of pressures and temperatures, and of solid He³ for pressures above the melting pressure. Some of their results are presented in Fig. 1. From these results we can conclude that the nuclear magnetic susceptibility of He³ can be represented, to a fair degree of approximation, by a Curie-Weiss law,

$$\chi(T) = C/(T + T_C); \quad T > T_C, \quad (1)$$

with a pressure dependent "paramagnetic" Curie temperature T_C given in Table I.

Figure 1 and Table I show that both solid and

TABLE I. Values of T_C obtained from the data in Fig. 1. on the basis of the definition: $\chi(T)T/C = \frac{1}{2}$ at $T = T_C$.

	p (atm)	T_C (°K)
liquid	0	≈ 0.2
liquid	25	≈ 0.1
solid	$\gtrsim 30$	≈ 0.1

† This work was partly done at the Ames Laboratory of the U. S. Atomic Energy Commission and was also supported in part at Washington University by the U. S. Air Force Office of Scientific Research.

¹ J. Pomeranchuk, Zhur. Eksp. i Theoret. Fiz. 20, 919 (1950).

² H. Primakoff, Bull. Am. Phys. Soc. 2, 63 (1957).

³ L. Goldstein, Ann. Phys. 8, 390 (1959).

⁴ N. Bernardes and H. Primakoff, Phys. Rev. Letters 3, 144 (1959).

⁵ N. Bernardes and H. Primakoff, Phys. Rev. Letters 2, 290 (1959).

⁶ W. M. Fairbank and G. K. Walters, Suppl. Nuovo cimento 9, 297 (1958).

liquid He^3 behave as "nuclear antiferromagnetics," i.e., $T_C > 0$. For the liquid, Table I indicates that the pressure coefficient of the Curie temperature, $(1/T_C) \times (dT_C/dp)$, is $-2 \times 10^{-2}/\text{atm}$. For the solid, on the other hand, no systematic data on the variation of T_C with pressure is available though Fairbank and Walters⁶ have on occasion observed susceptibilities corresponding to "nuclear ferromagnetic" behavior, i.e., to $T_C < 0$; unfortunately, the exact experimental conditions for occurrence of this effect are not known. From a theoretical point of view, since the forces between two He atoms at small distances are strongly repulsive, one can anticipate that under sufficiently high pressure the solid becomes a nuclear ferromagnetic and hence T_C becomes < 0 . Our calculations in fact indicate that a pressure of the order of 150 atm may be sufficient to produce such an effect [see Eq. (23) below]. It should, however, be admitted that the available experimental data on $\chi(T)$ for solid He^3 are not certain and it is even conceivable that solid He^3 is a nuclear ferromagnetic at all pressures above the melting pressure.

Before attempting a quantitative calculation of the nuclear magnetic properties of solid He^3 , we have to understand the mechanisms for spin alignment in this solid. There are two essentially spin dependent terms in the effective Hamiltonian of solid He^3 : (1) a spin-spin magnetic interaction, which gives rise to an energy per atom $\Delta E_1 \cong (z/2)(\mu^2/R^3)$, where z is the number of nearest neighbor atoms to a given atom in the solid, μ the nuclear magnetic moment, and R the nearest neighbor distance; (2) a "symmetry" or "exchange" interaction between nearest neighbor atoms which depends on the root mean square deviation, δ , of an atom from its lattice site and which gives rise to an energy per atom

$$\Delta E_2 \cong (z/2)[a_1 W(R, \delta) + a_2 U(R, \delta)] \exp[-\frac{3}{4}(R/\delta)^2],$$

where W and U are, respectively, the average kinetic energy and average potential energy per atom in the

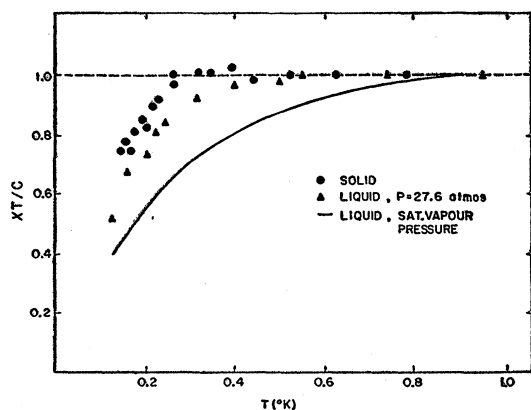


FIG. 1. Nuclear magnetic susceptibility χ of liquid He^3 and of solid He^3 as a function of temperature according to the measurements of Fairbank and Walters, reference 6.

solid, and the a 's are numerical constants whose absolute values are of the order of unity.

The spin-spin magnetic interaction, ΔE_1 , is the only term considered for the solid by Pomeranchuk¹ in his paper on liquid He^3 ; Pomeranchuk argues that "symmetry" or "exchange" effects, although important in the liquid, should be negligible in the solid, since here the atoms are bound to well-separated lattice sites ($\delta/R \ll 1$) so that the overlap between individual atom orbitals of neighbor atoms is negligible. From this argument Pomeranchuk concludes that, in the solid, spin alignment should not occur above a temperature $T_C \approx \Delta E_1 \cong (z/2)\mu^2/R^3$,⁷ which for solid He^3

$$[\mu = -2.1(e\hbar/2M_p c) = -1.1 \times 10^{-23} \text{ erg/gauss}, \\ R = 3.8 \text{ \AA}, z = 12^8]$$

is of the order of 10^{-7}°K . However, due to the small mass of the He^3 atom and to its weak binding within the solid lattice, δ/R is actually quite large in contrast to the heavier solids.^{9,10} Thus in solid He^3 the individual atom orbitals corresponding to nearest neighbors do have an appreciable overlap which produces an effective spin correlation much stronger than that due to the spin-spin magnetic interaction. This can be seen in a bit more quantitative detail, by using $\delta/R \approx \frac{1}{3}$, $W \approx -U \approx 10^\circ\text{K}$ (see Table II, p. 972), which gives $T_C \approx \Delta E_2 \approx 0.05^\circ\text{K}$. On the other hand, the above argument does not provide any information about the exact magnitude or even the sign of T_C , since as noted, $W \approx -U$ and since the signs of a_1 and a_2 cannot be predicted without a detailed calculation. However, we can conclude that symmetry or exchange effects represent the predominant mechanism for spin alignment in solid He^3 at low pressures, and our discussion will be concerned largely with the determination of the symmetry energy.

⁷ Here and below we choose our units in such a way that the Boltzmann constant k is a pure number equal to 1. Consequently energy will be expressed in $^\circ\text{K}$.

⁸ The value $R = 3.8 \text{ \AA}$ corresponds to an empirical value of 0.13 g/cm^3 for the density of solid He^3 at $T \lesssim 1^\circ\text{K}$ and $p \approx 30 \text{ atm}$ and to the assumption that the solid He^3 crystal lattice is close-packed cubic with $z = 12$, i.e., face-centered cubic, under these conditions. This assumption is consistent with the known lattice structures of solid Ne, Ar, Kr, Xe, and with the fact that the known lattice structures of the two forms of solid He^4 are also close-packed and is anticipated on the basis of the short-range character of the attractive Van der Waals forces among closed shell atoms. On the other hand, an experiment by A. F. Schuch, E. R. Grilly, and R. L. Mills [Phys. Rev. **110**, 775 (1958); see also E. R. Grilly and R. L. Mills, Ann. Phys. **8**, 1 (1959)] indicates that solid He^3 possesses a body-centered cubic lattice for $1.5^\circ\text{K} \lesssim T \lesssim 3^\circ\text{K}$ and $50 \text{ atm} \lesssim p \lesssim 130 \text{ atm}$; as mentioned just above, the existence of such a non-close-packed cubic lattice, at least for the states of lowest energy of solid He^3 , is difficult to understand from the point of view of the short range attractive character of the interatomic Van der Waals forces. The various results obtained below, while calculated for an assumed close-packed cubic lattice, are also expected to hold at least semiquantitatively for a body-centered cubic lattice.

⁹ N. Bernardes, Phys. Rev. **112**, 1534 (1958); Nuovo cimento **11**, 628 (1959), gives δ/R for solid Ne, Ar, Kr, Xe.

¹⁰ C. Domb and J. S. Dugdale, *Progress in Low-Temperature Physics*, edited by C. J. Gorter (North-Holland Publishing Company, Amsterdam, 1957), Vol. II, Chap. 11. These authors give δ/R for solid He^4 .

3. THE INTERATOMIC POTENTIAL

Within the general limitations of the Born-Oppenheimer approximation, it is possible to deduce the properties of gaseous, liquid, and solid He³ from the energy eigenfunctions and eigenvalues, $\Psi_n(\dots \mathbf{X}_k, S_k^{(z)}, \dots)$ and E_n , of the many-atom Schrödinger equation :

$$(H - E_n)\Psi_n = \left\{ \left[\frac{-\hbar^2}{2M} \sum_{k=1}^N \nabla_k^2 + \frac{1}{2} \sum_{i=1}^N \sum_{j=1}^N V(X_{ij}) + H'(\dots \mathbf{X}_k, S_k^{(z)}, \dots) \right] - E_n \right\} \times \Psi_n(\dots \mathbf{X}_k, S_k^{(z)}, \dots) = 0. \quad (2)$$

In Eq. (2) \mathbf{X}_k is the space coordinate of the center of mass of the k th atom, i.e., of the k th nucleus, and $S_k^{(z)}$ is the corresponding nuclear spin coordinate, ∇_k^2 is the Laplacian with respect to \mathbf{X}_k , $H'(\dots \mathbf{X}_k, S_k^{(z)}, \dots)$ is the interaction of the N -atom system with external forces such as an external magnetic field, the walls of a container which may exert an external pressure on the system, etc., and $V(X_{ij})$ is a spin independent, spherically symmetrical, phenomenological potential which can be considered as given and which ultimately reflects the Coulomb interaction between the nucleus and electrons of the i th atom and those of the j th atom. An explicit form for this phenomenological interatomic potential can be obtained from low-temperature gas-phase data, e.g., from the second virial coefficient.¹¹ In fact, it has been shown that the so-called Lennard-Jones "12-6" potential,

$$V(X_{ij}) = \frac{A}{X_{ij}^{12}} - \frac{B}{X_{ij}^6} = \epsilon(x_{ij}^{-12} - 2x_{ij}^{-6}) \equiv \epsilon v(x_{ij}), \quad (3)$$

where $r_0 x_{ij} \equiv X_{ij}$, and r_0 and ϵ are such that

$$(dV/dX)|_{X=r_0}=0, \quad \text{and} \quad V(r_0)=-\epsilon,$$

gives a good description of the gas-phase data of all inert elements and the solid-phase data of Ne, Ar, Kr, and Xe up to 20 000 atm.⁹

The main difficulty in finding the $\Psi_n(\dots \mathbf{X}_k, S_k^{(z)}, \dots)$ and E_n of Eq. (2) for solid He³ by the various standard approximation methods is connected with the strong singularity of the $V(X_{ij})$ of Eq. (3) at $X_{ij}=0$, i.e., with the strong interatomic repulsion at short distances. In order to eliminate divergences introduced by these various standard approximation methods, we modify the $V(X_{ij})$ by multiplication with an exponential factor

$$\exp(-\lambda x_{ij}^{-10}), \quad (4)$$

and discuss the eigenfunctions and eigenvalues of Eq. (2) with $V(X_{ij})$ replaced by an "effective" non-

singular interatomic potential

$$V_{\text{eff}}(X_{ij}) = \epsilon v(x_{ij}) \exp(-\lambda x_{ij}^{-10}), \quad (5)$$

where λ is a small parameter, $\lambda \ll 1$, whose exact value is determined below (see Sec. 5). The factor

$$\exp(-\lambda x_{ij}^{-10}),$$

chosen as such for calculational convenience, effectively modifies the $V(X_{ij})$ of Eq. (3) only at small interatomic distances— $X_{ij} \lesssim \lambda^{1/10} r_0$ —and consequently does not upset the fit to the low-temperature gas-phase data. We note that since the dominant spatial correlation of the atoms in solid He³ is to individual lattice points with nearest neighbor distance $R \cong \frac{1}{2} r_0$ (see Table II) and since in addition the Ψ_n are very small for X_{ij} appreciably less than r_0 ($\Psi_n \rightarrow 0$ faster than any power of X_{ij} as $X_{ij} \rightarrow 0$), we can write to a very good approximation:

$$E_n = \langle \Psi_n^* | H | \Psi_n \rangle \cong \langle \Psi_n^* | H_{\text{eff}} | \Psi_n \rangle,$$

where H_{eff} differs from the H of Eq. (2) by replacement of the $V(X_{ij})$ of Eq. (3) by the $V_{\text{eff}}(X_{ij})$ of Eq. (5).

4. SYMMETRY OR EXCHANGE EFFECTS

We now treat the symmetry or exchange effects in the energy eigenvalues of solid He³. For the ground-state energy eigenvalue of the solid, E_0 , with corresponding ground-state energy eigenfunction, Ψ_0 , we have

$$E_0 = \langle \Psi_0^* | H | \Psi_0 \rangle \cong \langle \Psi_0^* | H_{\text{eff}} | \Psi_0 \rangle \lesssim \langle \Phi_0^* | H_{\text{eff}} | \Phi_0 \rangle, \quad (6)$$

with Φ_0 , the variational-trial approximation to Ψ_0 : $\Phi_0 \approx \Psi_0$, expressed as a suitably antisymmetrized product of individual atom orbitals, $\varphi(\mathbf{X}_k - \mathbf{R}_i) \chi_{\pm \frac{1}{2}}(S_k^{(z)})$, localized on the various lattice points \mathbf{R}_i . Thus Φ_0 is a variational-trial wave function of the Heitler-London type. Further we use the Dirac vector model¹² for a quantitative description of the exchange effects. According to this model, if we consider: (1) the expectation values of the Hamiltonian operator

$$\begin{aligned} \langle H_{\text{eff}} \rangle_n &\equiv \langle \Phi_n^* | H_{\text{eff}} | \Phi_n \rangle \\ &\equiv \left\langle \Phi_n^* \left| \frac{-\hbar^2}{2M} \sum_{k=1}^N \nabla_k^2 + \frac{1}{2} \sum_{i=1}^N \sum_{j=1}^N V_{\text{eff}}(X_{ij}) \right| \Phi_n \right\rangle, \end{aligned} \quad (7)$$

the $\Phi_0 \approx \Psi_0$, $\Phi_1 \approx \Psi_1$, \dots , $\Phi_n \approx \Psi_n$, \dots

$$\left(\frac{1}{2} \sum_{i=1}^N \sigma_i \right)^2 \Phi_n = S_n(S_n + 1) \Phi_n$$

being ordered according to the eigenvalues of

$$\left(\frac{1}{2} \sum_{i=1}^N \sigma_i \right)^2$$

so that $\langle H_{\text{eff}} \rangle_0 < \langle H_{\text{eff}} \rangle_1 < \langle H_{\text{eff}} \rangle_2 < \dots$ but otherwise involving the same individual atom space orbitals

¹¹ See, for example, R. H. Fowler, *Statistical Mechanics* (Cambridge University Press, Cambridge, 1955), Chap. 10.

¹² P. A. M. Dirac, *The Principles of Quantum Mechanics* (Oxford University Press, New York, 1958), 4th ed., Chap. 9.

$\varphi(\mathbf{X}_k - \mathbf{R}_i)$; and (2) the corresponding ordered eigenvalues Ω_n of the equivalent Hamiltonian operator

$$\Omega \equiv K - \frac{1}{2} \sum_{i=1}^N \sum_{j=1}^N \frac{1}{2} J_{ij} (1 + \boldsymbol{\sigma}_i \cdot \boldsymbol{\sigma}_j), \quad (8)$$

we have the equality

$$\langle H_{\text{eff}} \rangle_n = \Omega_n, \quad (9)$$

where

$$K \equiv \int \cdots \int d\mathbf{X}_1 \cdots d\mathbf{X}_N \varphi^*(\mathbf{X}_1 - \mathbf{R}_1) \cdots \varphi^*(\mathbf{X}_N - \mathbf{R}_N) \\ \times \left[\frac{-\hbar^2}{2M} \sum_{k=1}^N \nabla_k^2 + \frac{1}{2} \sum_{i=1}^N \sum_{j=1}^N V_{\text{eff}}(X_{ij}) \right] \\ \times \varphi(\mathbf{X}_1 - \mathbf{R}_1) \cdots \varphi(\mathbf{X}_N - \mathbf{R}_N) \quad (10)$$

is the "volume energy" of the system of He³ atoms and

$$J_{ij} \equiv \int \int d\mathbf{X}_1 d\mathbf{X}_2 \varphi^*(\mathbf{X}_2 - \mathbf{R}_i) \varphi^*(\mathbf{X}_1 - \mathbf{R}_j) \\ \times \left[\frac{-\hbar^2}{2M} (\nabla_1^2 + \nabla_2^2) + V_{\text{eff}}(X_{12}) \right] \\ \times \varphi(\mathbf{X}_1 - \mathbf{R}_i) \varphi(\mathbf{X}_2 - \mathbf{R}_j) \quad (11)$$

is the "exchange integral" between the atoms at \mathbf{R}_i and \mathbf{R}_j . The quantity:

$$-\frac{1}{2} \sum_{i=1}^N \sum_{j=1}^N \frac{1}{2} J_{ij} (1 + \boldsymbol{\sigma}_i \cdot \boldsymbol{\sigma}_j)$$

is the "symmetry energy" or "exchange energy" of the system of He³ atoms. From the point of view of Eqs. (10), (11), the use of V_{eff} rather than V in K and J_{ij} may be viewed as roughly equivalent to the replacement of the atom pair potential energy operator by the corresponding scattering operator.

The equality of the indicated expectation values of H_{eff} and the corresponding eigenvalues of Ω [Eq. (9)] is rigorously valid only: (1) if the individual atom space orbitals in the K and in the J_{ij} of Ω are orthogonal; and (2) with the further neglect of terms in Ω arising from higher order permutations involving three or more atoms. However, Van Vleck¹³ and more recently Carr¹⁴ have presented "*a priori*" arguments showing that it is indeed plausible in Dirac vector model calculations to neglect *both* the nonorthogonality *and* the higher order permutation terms, and the success of theories of electronic ferro- and antiferromagnetism¹⁵ based on equations analogous to Eqs. (7)–(11) above constitutes a further, "*a posteriori*," justification.

¹³ J. H. Van Vleck, Phys. Rev. **49**, 232 (1936).

¹⁴ W. J. Carr, Phys. Rev. **92**, 28 (1953).

¹⁵ See, for example, the excellent review of J. Van Kranendonk and J. H. Van Vleck, Revs. Modern Phys. **30**, 1 (1958).

5. DETERMINATION OF V_{eff} AND CALCULATION OF THE VOLUME ENERGY

The volume energy K of Eqs. (8) and (10) may be written as:

$$K(V, \alpha; \lambda) = N \left(\frac{-\hbar^2}{2M} \right) \int d\mathbf{X} \varphi^*(\mathbf{X}) \nabla_{\mathbf{X}}^2 \varphi(\mathbf{X}) \\ + \frac{1}{2} \sum_{i=1}^N \sum_{j=1}^N \int \int d\mathbf{X} d\mathbf{X}' \varphi^*(\mathbf{X}) \varphi^*(\mathbf{X}') \\ \times V_{\text{eff}}(|\mathbf{X} - \mathbf{X}' + \mathbf{R}_i - \mathbf{R}_j|) \varphi(\mathbf{X}) \varphi(\mathbf{X}') \\ \equiv N \epsilon W_0 + N \epsilon U_0, \quad (12)$$

where V_{eff} is the "effective" interatomic potential of Eq. (5) which depends on the parameter λ , V is the volume which enters through the lattice spacing $|\mathbf{R}_i - \mathbf{R}_j|$, and α is a variational parameter appearing in the individual atom space orbitals which we take to be

$$\varphi(\mathbf{X}_k - \mathbf{R}_i) = (\text{const}) \exp[-\frac{1}{2}\alpha^2(\mathbf{X}_k - \mathbf{R}_i)^2].$$

Now in solid He³ most of the contribution to the (low-temperature) cohesive energy:

$$|E_0| \gtrsim |\langle \Phi_0^* | H_{\text{eff}} | \Phi_0 \rangle|$$

$$= |\Omega_0| = |K + \text{lowest eigenvalue of}$$

$$[-\frac{1}{4} \sum_{i=1}^N \sum_{j=1}^N J_{ij} (1 + \boldsymbol{\sigma}_i \cdot \boldsymbol{\sigma}_j)] \quad [\text{Eqs. (6)–(12)}]$$

comes from the volume energy K ; hence, in minimizing E_0 with respect to the variational parameter α , we may neglect the symmetry energy:

$$-\frac{1}{4} \sum_{i=1}^N \sum_{j=1}^N J_{ij} (1 + \boldsymbol{\sigma}_i \cdot \boldsymbol{\sigma}_j).$$

This follows since the cohesive energy per atom at zero pressure in solid He³ is only a little less than that in liquid He³ which is, empirically, $\cong 2.5$ °K¹⁶ while, again empirically,⁶ spin alignment in solid He³ first occurs at a temperature ≈ 0.1 °K which, according to Sec. 6 below, corresponds to a numerical value of $\approx \frac{1}{6}$ (0.1 °K) for the nearest neighbor J_{ij} . One can therefore, to a rather good approximation, find the optimum value α_0 of the variational parameter α , and hence the optimum individual atom space orbitals, $\varphi(\mathbf{X}) = (\text{const}) \times \exp[-\frac{1}{2}\alpha_0^2 \mathbf{X}^2]$, from the condition

$$(\partial/\partial\alpha) K(V, \alpha; \lambda) |_{\alpha=\alpha_0} = 0.$$

Thus the ground-state energy E_0 of solid He³ is given as a function of the volume V by $E_0(V, \alpha_0(V, \lambda); \lambda) \cong K(V, \alpha_0(V, \lambda); \lambda)$.

The volume energy $K(V, \alpha_0(V, \lambda); \lambda)$ and so

$$E_0(V, \alpha_0(V, \lambda); \lambda)$$

¹⁶ J. de Boer, *Progress in Low-Temperature Physics*, edited by C. J. Gorter (North-Holland Publishing Company, Amsterdam, 1957), Vol. II, Chap. 1.

TABLE II. Calculated ground-state energies and root mean square deviations obtained by the method described in the text.

R/r_0	$\alpha_0^2 r_0^2$	δ/R	W_0	U_0	K/Ne
Solid He ⁴ : $\epsilon=10.2$ °K, $r_0=2.88$ Å; $\lambda=1/15$					
1.19	8.8	0.35	0.93	-1.40	-0.47
1.24	8.6	0.34	0.91	-1.42	-0.51
1.28	8.4	0.33	0.89	-1.42	-0.53
1.32	8.2	0.32	0.87	-1.40	-0.53
1.38	8.0	0.31	0.85	-1.32	-0.47
Solid He ³ : $\epsilon=10.2$ °K, $r_0=2.88$ Å; $\lambda=1/15$					
1.19	7.0	0.39	0.99	-1.21	-0.22
1.24	6.9	0.38	0.97	-1.22	-0.25
1.28	6.8	0.37	0.96	-1.23	-0.27
1.32	6.6	0.36	0.92	-1.17	-0.25
1.38	6.4	0.35	0.90	-1.13	-0.23

still depend on the parameter λ which enters explicitly in Eq. (12) through the V_{eff} of Eq. (5) and implicitly through the dependence of α_0 on λ . In order to find a reasonable value for λ , we calculate the ground-state energy, $E_0(V, \alpha_0(V, \lambda); \lambda)$, and the mean square deviation of an atom from its lattice site,

$$\delta^2 \equiv \langle \Phi_0^* | (\mathbf{X}_i - \mathbf{R}_i)^2 | \Phi_0 \rangle \\ \cong \langle \varphi^* (\mathbf{X}_i - \mathbf{R}_i) | (\mathbf{X}_i - \mathbf{R}_i)^2 | \varphi (\mathbf{X}_i - \mathbf{R}_i) \rangle \\ = \frac{3}{2} [\alpha_0(V, \lambda)]^{-2},$$

for solid He⁴, where experimental values are known, using different values of λ and determine that λ which gives the best fit to the experimental values; this value of λ depends on α_0 and conversely α_0 may be considered as a function of λ so that one can also compare with experiment calculated values of α_0 (or δ) for various λ . We anticipate that the λ appropriate to solid He³ will be fairly close to that appropriate to solid He⁴ since the *actual* interatomic potential $V(X_{ij})$ is the *same* in He⁴ and in He³ and since the dominant spatial correlation of the atoms in either the ground state of solid He⁴ or in any of the states Φ_n in solid He³ is to individual lattice points.

Evaluation of $E_0(V, \alpha_0(V, \lambda); \lambda) \cong K(V, \alpha_0(V, \lambda); \lambda)$ and of $\delta(\alpha_0(V, \lambda))$ as a function of λ for solid He⁴ shows that $\lambda=1/15$ gives a fair description of these experimentally known¹⁶ properties of solid He⁴ at pressures ≈ 30 atm. The same value of λ used for solid He³ then yields the corresponding $E_0(V, \alpha_0(V, 1/15); 1/15)$ and $\delta(\alpha_0(V, 1/15))$. The numerical results are exhibited in Table II.

The results in Table II are obtained by a variational calculation with respect to the parameter α ; the lattice summation involved in Eq. (12) has been approximated by a summation over the first 42 neighbors in a close-packed cubic lattice (12 at a distance R , 6 at $R\sqrt{2}$ and 24 at $R\sqrt{3}$). The comparison with the experimental data is made by assuming the values adopted by de Boer¹⁶ for the parameters ϵ and r_0 , i.e., $\epsilon=10.2$ °K and $r_0=2.88$ Å for either of the two isotopes.

The approximate agreement in the case of solid He⁴ at pressures ≈ 30 atm between our results for $\lambda=1/15$

and experiment progressively disappears at higher pressures (smaller R/r_0). In particular, we predict too slow an increase of E_0 with pressure for solid He⁴ and so presumably for solid He³. Thus, it is clear that λ must actually decrease with increasing pressure as in fact one anticipates since the interatomic repulsion must become progressively more and more important in determining E_0 at higher pressures. This shortcoming of our procedure is however not serious for the present calculation since our interest is mainly to obtain at pressures ≈ 30 atm a reasonably good estimate of the exchange integral J_{ij} in Eq. (11). In a very rough fashion we can even give a discussion of several interesting phenomena in solid He³ at higher pressures, say 10^2 – 10^3 atm (see Sec. 6), by making a crude estimate of the variation of λ with pressure.

6. EXCHANGE INTEGRAL AND ITS DEPENDENCE ON PRESSURE

In the preceding section we obtained for solid He³ the ground-state energy and the root mean square deviation of an atom from its lattice site based on the assumption that symmetry or exchange effects are negligible. However, as we discussed in that section, even though the symmetry terms do not contribute appreciably to the ground-state energy, they nevertheless play an essential role in the determination of the magnetic properties.

According to Eqs. (7)–(11), we have to compute the exchange integrals J_{ij} of Eq. (11) which constitute the starting point for a calculation of the nuclear magnetic properties. Since the individual J_{ij} decrease rapidly with increasing separation between the lattice points \mathbf{R}_i and \mathbf{R}_j on which the individual atom orbitals are localized, we may approximate the summation over all pairs of atoms in Eq. (8) by a summation over nearest neighbors, i.e., approximate the symmetry energy as:

$$-\frac{1}{4} \sum_{i=1}^N \sum_{j=1}^N J_{ij} (1 + \boldsymbol{\sigma}_i \cdot \boldsymbol{\sigma}_j) \cong -\frac{1}{4} J \sum_{i=1}^N \sum_{j=1}^N \eta_{ij} (1 + \boldsymbol{\sigma}_i \cdot \boldsymbol{\sigma}_j) \\ = -\frac{1}{4} J N z - \frac{1}{4} J \sum_{i=1}^N \sum_{j=1}^N \eta_{ij} \boldsymbol{\sigma}_i \cdot \boldsymbol{\sigma}_j, \quad (13)$$

where $\eta_{ij}=1$ if i and j are nearest neighbors and $=0$ otherwise, and

$$J \equiv J \left(R, \alpha_0 \left(R, \frac{1}{15} \right); \frac{1}{15} \right) \\ = \int \int d\mathbf{X} d\mathbf{X}' \varphi^*(\mathbf{X}' - \mathbf{R}) \varphi^*(\mathbf{X}) \\ \times \left[\frac{-\hbar^2}{2M} (\nabla_{\mathbf{X}}^2 + \nabla_{\mathbf{X}'}^2) + V_{\text{eff}}(|\mathbf{X} - \mathbf{X}'|) \right] \\ \times \varphi(\mathbf{X} - \mathbf{R}) \varphi(\mathbf{X}') \equiv J_W + J_U, \quad (14)$$

$$J_W \equiv 2 \left(\frac{-\hbar^2}{2M} \right) \int d\mathbf{X} \varphi^*(\mathbf{X}) \nabla_{\mathbf{X}}^2 \varphi(\mathbf{X}-\mathbf{R}) \cdot \Delta, \quad (15)$$

$$J_U \equiv \int \int d\mathbf{X} d\mathbf{X}' \varphi^*(\mathbf{X}'-\mathbf{R}) \varphi^*(\mathbf{X}) \times V_{\text{eff}}(|\mathbf{X}-\mathbf{X}'|) \varphi(\mathbf{X}-\mathbf{R}) \varphi(\mathbf{X}'), \quad (16)$$

$$\Delta \equiv \int d\mathbf{X} \varphi^*(\mathbf{X}-\mathbf{R}) \varphi(\mathbf{X}). \quad (17)$$

The empirical value of the nearest neighbor distance R and the corresponding optimizing value of the variational parameter α are taken from Table II, and for a pressure of the order of 30 atm are: $R=3.80$ A = $1.32r_0$,^{8,17} $\alpha_0(R, 1/15)r_0 = (6.6)^{1/2} = 2.56$. Evaluating the integrals, Eq. (17) yields:

$$\Delta = \exp[-\frac{1}{4}(\alpha_0 r_0)^2 (R/r_0)^2] = \exp[-2.9], \quad (18)$$

and Eqs. (15), (18) give

$$J_W/\epsilon = 2W_0[1 - \frac{1}{6}(\alpha_0 r_0)^2 (R/r_0)^2] \Delta^2 = -5.4 \times 10^{-3}, \quad (19)$$

where $W_0 = \frac{3}{2}\hbar^2\alpha_0^2/2M\epsilon = 0.92$ is the average kinetic energy per atom defined in Eq. (12) and also listed in Table II. Thus, as may be anticipated from general arguments, the "exchange kinetic energy," J_W in Eq. (15), is *negative*. Further the "exchange potential energy," J_U in Eq. (16), can be written as

$$J_U/\epsilon = (\alpha_0 r_0)^3 \left\{ \left(\frac{2}{\pi} \right)^{\frac{1}{2}} \int_0^\infty dx x^2 (x^{-12} - 2x^{-6}) \times \exp[-\lambda x^{-10}] \exp[-\frac{1}{2}(\alpha_0 r_0)^2 x^2] \right\} \Delta^2 \\ \equiv (\alpha_0 r_0)^3 \{ I(\alpha_0 r_0; \lambda) \} \Delta^2. \quad (20)$$

For $\alpha_0(R, 1/15)r_0 = 2.56$ (see Table II) a numerical integration or an approximate analytical evaluation gives $I(2.56; 1/15) = 5.6 \times 10^{-2}$, so that Eq. (20) yields a *positive* exchange potential energy:

$$J_U/\epsilon = +3.2 \times 10^{-3}, \quad (21)$$

corresponding to the greater relative importance, even at $p \approx 30$ atm, of the repulsive term in V_{eff} . Equations (14), (19), and (21) show that J , the exchange integral between a pair of nearest neighbor atoms, is *negative*:

$$J = [-5.4 + 3.2] \times 10^{-3} \epsilon = -0.02 \text{ }^\circ\text{K}. \quad (22)$$

From the fact that the exchange integral is negative, so that the symmetry energy of Eqs. (8), (13) is:

$$+ \frac{1}{4} |J| \sum_{i=1}^N \sum_{j=1}^N \eta_{ij} (1 + \sigma_i \cdot \sigma_j),$$

¹⁷ The value of R appropriate to a pressure of 30 atm, R_{30} , is certainly less than the value of R appropriate to zero pressure which, from Table II, is $1.28r_0$. It is however more accurate to use an empirical value of $R_{30} = 3.80$ A = $1.32r_0$ as calculated from the empirical density at 30 atm obtained by an extrapolation of the molar volume data of E. R. Grilly and R. L. Mills [Ann. Phys. 8, 1 (1959)] which extends along the melting curve from 130 atm, 3.0°K to 50 atm, 1.3°K.

we conclude that the nuclear spins of neighboring He³ atoms effectively align in *opposite* directions in energetically low-lying states of the solid, i.e., we conclude that solid He³ behaves as a nuclear antiferromagnetic at sufficiently low temperatures. At temperatures $T \approx T_C = (z/2)|J| = 6|J|$ [see Eq. (37) below] this spin correlation will be destroyed by thermal agitation; using Eq. (22), $T_C = 6|J| \approx 0.1$ °K, which is close to the value indicated by the susceptibility measurements of Fairbank and Walters.⁶ Similar theoretical results for T_C have been obtained by Primakoff² on the basis of a different model for the calculation of the symmetry energy. On the other hand, and as we have already noted, Pomeranchuk¹ predicts $T_C \approx 10^{-7}$ °K in a treatment where only the spin-spin magnetic interaction energy is considered.

The value of the exchange integral J , given by Eq. (22), is obtained by using values of R and $\alpha_0(R, 1/15)$ in Eqs. (14)–(21) appropriate to a pressure $p \approx 30$ atm. We have also estimated the pressure dependence of $J(R(p), \alpha_0(R(p), \lambda(p)); (\lambda p))$ on the basis of simple assumptions regarding the decrease of λ (below $1/15$) with increase of p (beyond 30 atm) and we find¹⁸

$$\frac{1}{J} \frac{dJ}{dp} = -\frac{1}{T_C} \frac{dT_C}{dp} \approx -1 \times 10^{-2} / \text{atm}. \quad (23)$$

Equation (23) indicates that for pressures $\gtrsim (30+100)$ atm = 130 atm the exchange integral J is *positive* so that for such higher pressures the energetically low-lying states of the solid correspond to alignment of neighboring nuclear spins in the *same* direction. Thus solid He³ may be expected to behave as a nuclear ferromagnetic ($T_C < 0$) at sufficiently low temperatures ($T \lesssim 0.1$ °K) and high pressures ($p \gtrsim 150$ atm)—a possibility by no means excluded by the available experimental evidence (see Sec. 2). In fact, our prediction of a nuclear antiferromagnetic to nuclear ferromagnetic transition for $p \approx 150$ atm and $T \lesssim 0.1$ °K could be connected with the crystallographic transition observed by Grilly and Mills¹⁷ at pressures ≈ 100 atm so that the low-pressure stable (α : close-packed cubic⁸) and the high-pressure stable (β : close-packed hexagonal) crystal structures in solid He³ may conceivably be characterized by $T_C > 0$ and $T_C < 0$, respectively.¹⁸

7. NUCLEAR MAGNETIC SUSCEPTIBILITY AND SPECIFIC HEAT OF SOLID He³

Having obtained both the volume energy K and the exchange integral J in the symmetry energy and so having specified the equivalent Hamiltonian Ω [Eqs. (8)–(22)], we proceed to calculate the (Helmholtz) free energy of solid He³ in an external magnetic field, $F(T, V, B)$:

$$\exp[-F(T, V, B)/T] \\ = \sum_{\text{all states: } \nu} \exp[-E_\nu(V, B)/T]. \quad (24)$$

¹⁸ To be published.

Once $F(T, V, B)$ is known we can obtain the nuclear magnetization M , the entropy S , and the specific heat at constant volume and constant field C_V , by means of the usual formulas of statistical thermodynamics, viz.,

$$M(T, V, B) = -\frac{\partial F(T, V, B)}{\partial B}, \quad (25)$$

$$S(T, V, B) = -\frac{\partial F(T, V, B)}{\partial T}, \quad (26)$$

$$C_V(T, V, B) = T \frac{\partial S(T, V, B)}{\partial T} = -T \frac{\partial^2 F(T, V, B)}{\partial T^2}. \quad (27)$$

Also, for $T \approx T_C$, and $B \ll T_C/\mu$, M is, to a very good approximation, linear in B so that the nuclear magnetic susceptibility is given by

$$\chi(T, V, B) \equiv \frac{\partial M(T, V, B)}{\partial B} = -\frac{\partial^2 F(T, V, B)}{\partial B^2} \Big|_{B=0} \cong -\left\{ \frac{\partial^2 F(T, V, B)}{\partial B^2} \right\}_{B=0} = \chi(T, V, 0). \quad (28)$$

In view of our previous discussion in Secs. 1, 4-6, we can approximately decompose the energy $E_\nu(V, B)$ of any state ν of the solid He^3 into: (1) the volume energy $E_{\text{vol}}(R) \equiv K(R, \alpha_0(R, 1/15); 1/15)$; (2) the symmetry plus spin orientation energy $E_{\text{sp}, \nu}(R, B) \equiv$ an eigenvalue of

$$-\frac{1}{4}J \left(R, \alpha_0 \left(R, \frac{1}{15} \right); \frac{1}{15} \right) \sum_{i=1}^N \sum_{j=1}^N \eta_{ij} (1 + \sigma_i \cdot \sigma_j) - \mu B \sum_{i=1}^N \sigma_i^{(z)};$$

and (3) the lattice vibration or phonon energy,¹⁹

$$E_{\text{ph}, \nu}(R) = \sum_{\mathbf{k}, \xi} n_\nu(\mathbf{k}, \xi) \hbar \omega_{\mathbf{k}, \xi}(R).$$

We thus have,

$$E_\nu(V, B) \cong E_{\text{vol}}(R) + E_{\text{sp}, \nu}(R, B) + E_{\text{ph}, \nu}(R); \quad V = NR^3/\sqrt{2}. \quad (29)$$

In view of Eq. (29) we can write Eqs. (24)-(28) as:

$$\begin{aligned} \exp[-F(T, V, B)/T] &= \exp[-E_{\text{vol}}(R)/T] \sum_{\text{sp. states: } \nu} \exp[-E_{\text{sp}, \nu}(R, B)/T] \\ &\quad \times \sum_{\text{ph. states: } \nu} \exp[-E_{\text{ph}, \nu}(R)/T] \\ &= \exp[-F_{\text{vol}}(V)/T] \exp[-F_{\text{sp}}(T, V, B)/T] \\ &\quad \times \exp[-F_{\text{ph}}(T, V)/T], \quad (30) \end{aligned}$$

¹⁹ \mathbf{k} = phonon wave number; ξ = phonon polarization index; $\omega_{\mathbf{k}, \xi}(R)$ = phonon frequency; $n_\nu(\mathbf{k}, \xi)$ = number of phonons with wave number \mathbf{k} , polarization ξ in state ν .

$$M(T, V, B) = -\frac{\partial F_{\text{sp}}(T, V, B)}{\partial B}, \quad (31)$$

$$\begin{aligned} S(T, V, B) &= S_{\text{sp}}(T, V, B) + S_{\text{ph}}(T, V) \\ &= -\frac{\partial F_{\text{sp}}(T, V, B)}{\partial T} - \frac{\partial F_{\text{ph}}(T, V)}{\partial T}, \quad (32) \end{aligned}$$

$$\begin{aligned} C_V(T, V, B) &= C_{\text{sp}}(T, V, B) + C_{\text{ph}}(T, V) \\ &= -T \frac{\partial^2 F_{\text{sp}}(T, V, B)}{\partial T^2} - T \frac{\partial^2 F_{\text{ph}}(T, V)}{\partial T^2}, \quad (33) \end{aligned}$$

$$\chi(T, V, 0) = -\left\{ \frac{\partial^2 F_{\text{sp}}(T, V, B)}{\partial B^2} \right\}_{B=0}. \quad (34)$$

Two different mathematical methods may now be used in the evaluation of the free energy of the nuclear spins,

$$\begin{aligned} \exp[-F_{\text{sp}}(T, V, B)/T] &= \sum_{\text{sp. states: } \nu} \exp[-E_{\text{sp}, \nu}(R, B)/T] \\ &= \text{Trace} \left\{ \exp \left[-\frac{1}{4} \frac{J(R)}{T} \sum_{i=1}^N \sum_{j=1}^N \eta_{ij} (1 + \sigma_i \cdot \sigma_j) \right. \right. \\ &\quad \left. \left. + \frac{\mu B}{T} \sum_{i=1}^N \sigma_i^{(z)} \right] \right\}, \quad (35) \end{aligned}$$

the first in the case of "high" temperatures, and the second in the case of "low" temperatures. In the "low"-temperature region the spin-wave method, as described for instance by Van Kranendonk and Van Vleck,¹⁵ is reasonably satisfactory for calculating $F_{\text{sp}}(T, V, B)$, while for "high" temperatures there exist several different though related procedures for approximately evaluating $F_{\text{sp}}(T, V, B)$; we shall use a method proposed by Kramers, and developed by Opechowski.²⁰

The Kramers-Opechowski method to evaluate $F_{\text{sp}}(T, V, B)$ in Eq. (35) involves the expression of $-T \ln \text{Trace} \{ \dots \}$ as a series expansion in J/T which converges rather rapidly for $T \gg |J|$. Adapting the results of Kramers and Opechowski to our purpose we can write

$$\begin{aligned} \frac{F_{\text{sp}}(T, V, B)}{NJ} &= -\frac{z}{4} \frac{1}{\gamma} \left[\ln 2 + \frac{\gamma^2 b^2}{2} + \dots \right] - \frac{z}{4} \gamma^2 b^2 \\ &\quad - (z/16) \gamma [3 + 2(z-2) \gamma^2 b^2 + \dots] \\ &\quad + A_3(\gamma b) \gamma^2 + A_4(\gamma b) \gamma^3 + \dots, \quad (36) \end{aligned}$$

where $\gamma \equiv J/T$ and $b \equiv \mu B/J$. The higher order terms in γ , $A_3(\gamma b) \gamma^2$, $A_4(\gamma b) \gamma^3$, \dots , constitute a relatively small correction for $T \gg |J|$ and are neglected below.

²⁰ W. Opechowski, *Physica* 4, 181 (1937).

Equations (36) and (34) give:

$$\begin{aligned}\chi(T, V, 0) &= \frac{N\mu^2}{J} \gamma \left[1 + \left(\frac{z}{2} \right) \gamma + \left(\frac{z-2}{z} \right) \left(\frac{z}{2} \right)^2 \gamma^2 \right] \\ &\cong \frac{N\mu^2}{J} \gamma / (1 - \frac{1}{2} z \gamma) \\ &= N\mu^2 / (T - \frac{1}{2} z J). \quad (37)\end{aligned}$$

Equation (37) is just the Curie-Weiss law with $T_C = -(z/2)J$, i.e., in the case of a close-packed lattice, $T_C = -6J$. From Eqs. (37) and (22) we conclude that solid He³ is a nuclear antiferromagnetic at pressures ≈ 30 atm, with a "paramagnetic" Curie temperature $T_C \cong 6 \times 0.02$ °K = 0.1 °K. Experimental results of Fairbank and Walters⁶ (see our Table I and Fig. 1) indicate that T_C is indeed close to 0.1 °K for $p \approx 30$ atm.

We can also use Eqs. (32), (33), and (36) to calculate the entropy and the specific heat of the nuclear spins. We obtain, considering the case of no external magnetic field, $b=0$,

$$S_{sp}(T, V, 0) = N(\ln 2 - T_C^2/16T^2); \quad T \gg T_C, \quad (38)$$

$$C_{sp}(T, V, 0) = NT_C^2/8T^2; \quad T \gg T_C. \quad (39)$$

These results are valid only in the "high"-temperature region, $T \gg T_C$. In the "low"-temperature region, $T \ll T_C$, $F_{sp}(T, V, 0)$, $S_{sp}(T, V, 0)$, $C_{sp}(T, V, 0)$, etc., can be obtained by a suitable adaptation of the spin-wave method as follows.

According to the two sublattice model of antiferromagnetism treated in the spin-wave approximation¹⁵ the eigenvalues, $E_{sp;\nu}(R, 0)$, of the symmetry energy:

$$\frac{1}{4} |J(R)| \sum_{i=1}^N \sum_{j=1}^N \eta_{ij} (1 + \sigma_i \cdot \sigma_j)$$

are given by

$$E_{sp;\nu}(R, 0) = E_{sp;0}(R, 0) + \sum_{\mathbf{k}} [n_{\nu}^{(1)}(\mathbf{k}) \hbar \omega_{\mathbf{k}}^{(1)}(R) + n_{\nu}^{(2)}(\mathbf{k}) \hbar \omega_{\mathbf{k}}^{(2)}(R)], \quad (40)$$

where $E_{sp;0}(R, 0)$ is the spin-wave zero point energy, \mathbf{k} , $\omega_{\mathbf{k}}^{(1)}(R)$, $\omega_{\mathbf{k}}^{(2)}(R)$ the spin-wave wave numbers and corresponding frequencies, and $n_{\nu}^{(1)}(\mathbf{k})$, $n_{\nu}^{(2)}(\mathbf{k})$ the numbers of spin-wave quanta or magnons with wave number \mathbf{k} present in the state ν . Equations (40), (35) yield:

$$\begin{aligned}F_{sp}(T, V, 0) &= E_{sp;0}(R, 0) \\ &+ T \sum_{\mathbf{k}} \{ \ln[1 - \exp[-\hbar \omega_{\mathbf{k}}^{(1)}(R)/T]] \\ &+ \ln[1 - \exp[-\hbar \omega_{\mathbf{k}}^{(2)}(R)/T]] \}. \quad (41)\end{aligned}$$

In the case of zero external magnetic field, and with neglect of anisotropy, the spin-wave frequencies are degenerate: $\omega_{\mathbf{k}}^{(1)}(R) = \omega_{\mathbf{k}}^{(2)}(R) \equiv \omega_{\mathbf{k}}(R)$. Further, at "low" temperatures, $T \ll T_C$, only spin waves with small wave number $|\mathbf{k}|$ are excited, and for these we

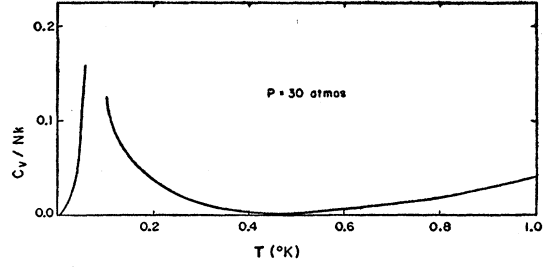


Fig. 2. Specific heat C_V of solid He³ as a function of temperature at a pressure \gtrsim melting pressure in the indicated temperature range calculated from Eqs. (33), (39), (45), (46).

can write.¹⁵

$$\hbar \omega_{\mathbf{k}}(R) \cong (z/\sqrt{3}) |J(R)| |\mathbf{k}| R, \quad (42)$$

where, as before, R is the nearest neighbor distance.

Equations (40)–(42) are derived on basis of a two simple-cubic sublattice model which is applicable, for instance, to a body-centered cubic lattice where $z=8$; we assume, however, that these equations are also approximately valid with $z=12$ for a close-packed cubic, i.e., face-centered cubic lattice. Then, substituting Eqs. (40), (42) into Eq. (41) and using

$$\sum_{\mathbf{k}} \dots = \frac{NR^3/\sqrt{2}}{(2\pi)^3} \int d\mathbf{k} \dots,$$

we obtain, for $T \ll 6|J| = T_C$,

$$\frac{F_{sp}(T, V, 0)}{|J|} = \frac{E_{sp;0}(R, 0)}{|J|} - N[0.6(T/T_C)^4]. \quad (43)$$

Thus, from Eqs. (43), (32), (33),

$$S_{sp}(T, V, 0) = N[0.4(T/T_C)^3]; \quad T \ll T_C, \quad (44)$$

$$C_{sp}(T, V, 0) = N[1.2(T/T_C)^3]; \quad T \ll T_C. \quad (45)$$

Equations (45), (39)—see also plot in Fig. 2—describe the specific heat of the nuclear spins at temperatures $T \ll T_C \cong 0.1$ °K and $T \gg T_C \cong 0.1$ °K, respectively. Preliminary data of Brewer, Sreedhar, Kramers, and Daunt²¹ seem to indicate a strong deviation of the measured specific heat of solid He³ from the T^3 law of the Debye phonon model at temperatures $T \cong 0.1$ °K; this deviation, if further confirmed, will constitute at least a qualitative experimental verification of the above predicted $C_{sp}(T, V, 0)$.

In concluding the present section it is important to note that the specific heat, the thermal expansion coefficient and the susceptibility of solid He³ are expected, in our approximation [Eqs. (33), (39), (45), (46), (34), (36), (37), (52), (53)], to exhibit "singularities"—e.g., cusp-like or otherwise well-defined maxima—at $T \approx T_C$ while no such singularities (at $T \approx T_C$) are found in the specific heat,²² the thermal expansion

²¹ D. F. Brewer, A. K. Sreedhar, H. C. Kramers, and J. G. Daunt, *Physica* **24**, S132 (1958).

²² D. F. Brewer, J. G. Daunt, and A. K. Sreedhar, *Phys. Rev.* **115**, 836 (1959).

coefficient²³ and the susceptibility⁶ of liquid He³—in this connection the apparent sharp break in the χT vs T curve of solid He³ (see Fig. 1) is to be noted. This predicted striking difference in the thermodynamic behavior of the two phases is ultimately to be ascribed to the difference in the spatial correlation of the atoms in the solid and in the liquid which implies a corresponding difference in the character of the associated quasiparticles (magnons and phonons in the solid; individual atoms with $M_{\text{eff}} \neq M$ in the liquid). This last difference in turn implies a difference in the corresponding energy level densities and so a difference in the “degrees of smoothness” (as a function of T, V, B) of the appertaining free energies.

8. ENTROPY OF SOLID He³ AS A FUNCTION OF PRESSURE AND THE COEFFICIENT OF THERMAL EXPANSION

With the nuclear spin or magnon entropy of solid He³ given in Eqs. (38) and (44) we next calculate the lattice vibration or phonon entropy of solid He³ and also the corresponding specific heat; Eqs. (29), (30), (32), (33) yield the standard results of the Debye model:

$$S_{\text{ph}}(T, V) = N[80(T/T_D)^3];$$

$$C_{\text{ph}}(T, V) = N[240(T/T_D)^3]; \quad T \ll T_D, \quad (46)$$

where $T_D \equiv \hbar\{\omega_{k,\xi}(R)\}_{\text{max}}$ is the Debye temperature; quantitatively, $T_D \cong 2\epsilon W_0$,⁹ so that in view of Eq. (12), the discussion just below Eq. (19), and Table II, $T_D \cong 20^\circ\text{K}$.

Thus at “high” temperatures ($T_c \ll T \ll T_D$) or at “low” temperatures, ($T \ll T_c \ll T_D$), the total entropy is given by [Eqs. (46), (44), (38), (32)]

$$S(T, V, 0) = N \left[\ln 2 - \frac{1}{16} \left(\frac{T_c}{T} \right)^2 + 80 \left(\frac{T}{T_D} \right)^3 \right];$$

$$T_c \ll T \ll T_D, \quad (47)$$

$$S(T, V, 0) = N \left[0.4 \left(\frac{T}{T_c} \right)^3 + 80 \left(\frac{T}{T_D} \right)^3 \right]$$

$$\cong N \left[0.4 \left(\frac{T}{T_c} \right)^3 \right]; \quad T \ll T_c \ll T_D, \quad (48)$$

so that the phonon entropy is negligible compared to the magnon entropy at “low” temperatures.

Now one of the Maxwell thermodynamic relations,

$$\frac{\partial S(T, p, 0)}{\partial p} = - \frac{\partial V(T, p, 0)}{\partial T}, \quad (49)$$

implies that the isobaric thermal expansion coefficient, $\alpha(T, p, 0) = [1/V(T, p, 0)][\partial V(T, p, 0)/\partial T]$, is positive or negative according to whether the entropy decreases or increases with pressure along an isothermal. Hence,

²³ D. F. Brewer and J. G. Daunt, Phys. Rev. **115**, 843 (1959).

from Eqs. (47)–(49), we have:

$$\frac{\partial V(T, p, 0)}{\partial T} = - \frac{\partial S(T, p, 0)}{\partial p} = N \left[\frac{1}{8} \left(\frac{T_c}{T} \right)^2 \left(\frac{1}{T_c} \frac{dT_c}{dp} \right) \right. \\ \left. + 240 \left(\frac{T}{T_D} \right)^3 \left(\frac{1}{T_D} \frac{dT_D}{dp} \right) \right];$$

$$T_c \ll T \ll T_D, \quad (50)$$

$$\frac{\partial V(T, p, 0)}{\partial T} = - \frac{\partial S(T, p, 0)}{\partial p} = N \left[1.2 \left(\frac{T}{T_c} \right)^3 \left(\frac{1}{T_c} \frac{dT_c}{dp} \right) \right. \\ \left. + 240 \left(\frac{T}{T_D} \right)^3 \left(\frac{1}{T_D} \frac{dT_D}{dp} \right) \right];$$

$$T \ll T_c \ll T_D, \quad (51)$$

where, numerically,

$$[(1/T_c)(dT_c/dp)] = -1 \times 10^{-2}/\text{atm} \quad [\text{Eq. (23)}];$$

$$[(1/T_D)(dT_D/dp)] = [-(d \log T_D)/(d \log V(0, p, 0))] \\ \times [- (d \log V(0, p, 0)/(dp))] \equiv (\gamma)(\beta)$$

(γ = Gruneisen's constant; β = isothermal compressibility at $T = 0^\circ\text{K}$) $\cong (1.5)(3 \times 10^{-3}/\text{atm})^{9,17}$; $T_c \cong 0.1^\circ\text{K}$ [Eqs. (37), (22)]; $T_D \cong 20^\circ\text{K}$ [Eq. (46) ff.]; $V(T, p, 0) \cong V(0, 30 \text{ atm}, 0) \cong 24 \text{ cm}^3/\text{mole}^{8,17}$. Thus, Eqs. (50), (51) yield

$$\alpha(T, p, 0) \cong (-5 \times 10^{-5} T^{-2} + 4.5 \times 10^{-4} T^3);$$

$$T_c \ll T \ll T_D, \quad (52)$$

$$\alpha(T, p, 0) \cong (-42 T^3 + 4.5 \times 10^{-4} T^3); \quad T \ll T_c \ll T_D. \quad (53)$$

From Eq. (53) we see that the magnitudes of the coefficients of thermal expansion of solid He³ and solid He⁴ below 0.1°K should differ by a factor of the order of $10^5(42/4.5 \times 10^{-4})$.

The isobaric thermal expansion coefficient of solid He³, $\alpha(T, p, 0)$, as given by Eqs. (52) and (53), is shown in Fig. 3 as a function of temperature. From Fig. 3 we see that this coefficient is negative below about

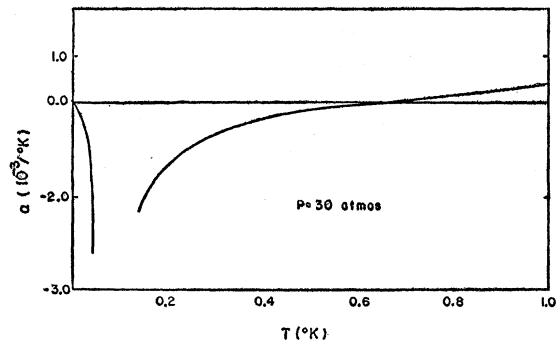


FIG. 3. Thermal expansion coefficient α of solid He³ as a function of temperature at a pressure \gtrsim melting pressure in the indicated temperature range calculated from Eqs. (52), (53).

0.6 °K, and exhibits an anomaly near $T_c \cong 0.1$ °K. We emphasize again that all the results of this section hold only for temperatures below 1 °K and for pressures ≈ 30 atm.

The isobaric thermal expansion coefficient, $\alpha(T, p, 0)$, is connected to the temperature change, $(\Delta T)_s$, occurring under isentropic compression or expansion by the thermodynamic relation:

$$\begin{aligned} \alpha(T, p, 0) &= \frac{1}{V(T, p, 0)} \frac{\partial V(T, p, 0)}{\partial T} = - \frac{1}{V(T, p, 0)} \frac{\partial S(T, p, 0)}{\partial p} \\ &= \left(\frac{1}{VT} \right) \left(T \frac{\partial S(T, p, 0)}{\partial T} \right) \left(\frac{\partial T(p, S, 0)}{\partial p} \right) \\ &= \frac{C_p(T, p, 0)}{VT} \frac{(\Delta T)_s}{(\Delta p)_s}. \quad (54) \end{aligned}$$

Thus for $(\Delta p)_s > 0$ —isentropic compression— $(\Delta T)_s$ has the same sign as $\alpha(T, p, 0)$ so that in view of Eqs. (52), (53) and Fig. 3 it should be possible to cool solid He³ by an isentropic compression if the initial temperature is less than $\cong 0.6$ °K. It should also be mentioned that Eq. (54) has been used by Brewer and Daunt²³ to obtain, in liquid He³, calculated values of $\alpha(p, T, 0)$ from measured values of $(\Delta T)_s/(\Delta p)_s$, and this method could be employed as well in solid He³. In addition Fairbank and Walters⁶ have observed that in an isentropic expansion of the solid into the liquid— $(\Delta p)_s < 0$ —“heating occurs at the melting point for T below about 0.4 °K and cooling occurs above this temperature,” i.e., the corresponding $(\Delta T)_s > 0$ for $T \lesssim 0.4$ °K. This finding however does not constitute unambiguous evidence for $\alpha(T, p, 0) < 0$ for $T \lesssim 0.4$ °K since $(\Delta T)_s$ is necessarily positive in this type of experiment if, for example, $S_{\text{sol}}(T, p, 0) - S_{\text{liq}}(T, p, 0)$ is positive and sufficiently large for $T \lesssim 0.4$ °K (see Sec. 9). It is thus clear that isentropic expansion or compression experiments are necessary at various temperatures within the solid phase *alone* to settle [via Eq. (54)] the question of the sign of the thermal expansion coefficient of solid He³.

Finally, it is of some interest to give the numerical value of $(\Delta T)_s/T(\Delta p)_s$ as anticipated from Eq. (54). Confining ourselves to the case: $T \ll T_c \ll T_D$, Eqs. (45), (46), (51), (53) yield

$$\begin{aligned} C_p(T, p, 0) &\cong C_V(T, V, 0) \cong C_{\text{sp}}(T, V, 0) = N[1.2(T/T_c)^3], \\ \alpha(T, p, 0) &\cong \frac{N}{V} \left[1.2 \left(\frac{T}{T_c} \right)^3 \left(\frac{1}{T_c} \frac{dT_c}{dp} \right) \right] \\ &\cong \frac{C_p(T, p, 0)}{V} \left(\frac{1}{T_c} \frac{dT_c}{dp} \right), \quad (55) \end{aligned}$$

so that, from Eqs. (54), (23),

$$\frac{(\Delta T)_s}{T(\Delta p)_s} \cong \frac{1}{T_c} \frac{dT_c}{dp} \cong -1 \times 10^{-2} / \text{atm}. \quad (56)$$

This approximate equality of $(\Delta T)_s/T(\Delta p)_s$ and $(1/T_c)(dT_c/dp)$ is, of course, solely a consequence of the fact that for $T \ll T_c \ll T_D$ the phonon entropy is negligible and hence

$$S(T, p, 0) \cong S_{\text{sp}}(T, p, 0) = S_{\text{sp}}(T/T_c(p)).$$

Thus, we have

$$\begin{aligned} \Delta S &= \frac{\partial S(T, p, 0)}{\partial T} \Delta T + \frac{\partial S(T, p, 0)}{\partial p} \Delta p = \frac{\partial S(T, p, 0)}{\partial T} \Delta T \\ &\quad + \frac{\partial S(T, p, 0)}{\partial T_c} \frac{dT_c}{dp} \Delta p = \frac{\partial S(T, p, 0)}{\partial T} \Delta T \\ &\quad - \frac{T}{T_c} \frac{\partial S(T, p, 0)}{\partial T} \frac{dT_c}{dp} \Delta p, \end{aligned}$$

whence, in an isentropic change— $\Delta S = 0$ —

$$\frac{(\Delta T)_s}{T(\Delta p)_s} \cong \frac{1}{T_c} \frac{dT_c}{dp}.$$

9. MELTING CURVE OF He³

Since $\chi_{\text{sol}}(T, p, 0) > \chi_{\text{liq}}(T, p, 0)$ for 0.1 °K $\lesssim T \lesssim 0.4$ °K and $p \approx p_{\text{melt}}$ (Fig. 1) we expect that for these temperatures solid He³ has less spin alignment and so more entropy than liquid He³; since at higher temperatures the entropy of the liquid is greater than that of the solid, the melting curve— p_{melt} vs T_{melt} —should have a minimum for $T_{\text{melt}} \approx 0.4$ °K. If this is true one can, as first pointed out by Pomeranchuk,¹ for instance

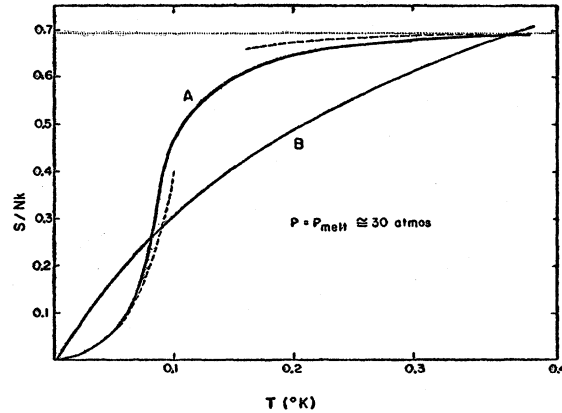


FIG. 4. Curve A: entropy of solid He³ from Eqs. (47), (48) with suitable interpolation near $T_c = 0.1$ °K. Curve B: entropy of liquid He³ from experiment (reference 23). Both of these entropies are plotted as functions of temperature along the melting curve. The horizontal dotted line corresponds to: entropy of solid He³ = $Nk \ln 2$ and is appropriate to $T_c < 10^{-6}$ °K.

melt solid He³ by decreasing its temperature at constant pressure for appropriate values of pressure and initial temperature. Direct information bearing on such an unusual thermodynamic behavior is clearly of considerable interest.

At the present stage of development of the theory of solid He³ and liquid He³ it is not possible to calculate the melting curve wholly from first principles. However, one can construct a relevant part of the melting curve of He³ from the knowledge of: (1) the entropy, $\{S_{\text{sol}}(T, p, 0)\}_{\text{melt}} \cong S_{\text{sol}}(T, p=30 \text{ atm}, 0)$, of the solid along the melting curve: our Eqs. (47) and (48) suitably interpolated near T_C ; (2) the entropy, $\{S_{\text{liq}}(T, p, 0)\}_{\text{melt}}$, of the liquid along the melting curve: from the experiments of Brewer and Daunt²³ at several pressures, first suitably extrapolated to $p=30 \text{ atm}$ and then to $p_{\text{melt}}(T_{\text{melt}}, 0)$; (3) the Clausius-Clapeyron equation

$$\left\{ \frac{dp(T, 0)}{dT} \right\}_{\text{melt}} = \frac{\{S_{\text{liq}}(T, p, 0)\}_{\text{melt}} - \{S_{\text{sol}}(T, p, 0)\}_{\text{melt}}}{\{V_{\text{liq}}(T, p, 0)\}_{\text{melt}} - \{V_{\text{sol}}(T, p, 0)\}_{\text{melt}}} = \frac{\{\Delta S(T, p, 0)\}_{\text{melt}}}{\{\Delta V(T, p, 0)\}_{\text{melt}}},$$

i.e.,

$$p_{\text{melt}}(T_{\text{melt}}, 0) = p_0 + \int_{T_0}^{T_{\text{melt}}} \frac{\{\Delta S(T, p, 0)\}_{\text{melt}}}{\{\Delta V(T, p, 0)\}_{\text{melt}}} dT, \quad (57)$$

(4) $\{\Delta V(T, p, 0)\}_{\text{melt}} \cong \Delta V(T_0, p_0, 0) \cong 1 \text{ cm}^3/\text{mole}^{17}$; (5) $T_0 \equiv$ melting temperature for which $\{\Delta S\}_{\text{melt}} = 0$; $T_0 = 0.37 \text{ }^\circ\text{K}$ from Fig. 4; $p_0 \equiv$ corresponding melting pressure, assumed = 29.1 atm for best over-all fit with experiment. Figure 4 shows $\{S_{\text{liq}}(T, p, 0)\}_{\text{melt}}$ (curve B), and $\{S_{\text{sol}}(T, p, 0)\}_{\text{melt}} \cong S_{\text{sol}}(T, p=30 \text{ atm}, 0)$, the latter for two different values of T_C : (a) $T_C = 0.1 \text{ }^\circ\text{K}$ as given by Eqs. (37) and (22) and by the susceptibility measurements of Fairbank and Walters⁶ (curve A); and (b) $T_C < 10^{-6} \text{ }^\circ\text{K}$ i.e., $T_C = 10^{-7} \text{ }^\circ\text{K}$ as suggested by Pomeranchuk¹ (horizontal dotted line).

The melting curves for $T < 0.5 \text{ }^\circ\text{K}$, calculated from

Eq. (57) and Fig. 4 with the two quoted values of T_C , are presented in Fig. 5 together with typical experimental points obtained by Baum, Brewer, Daunt, and Edwards.²⁴ Agreement between the melting curve obtained with our $T_C = 0.1 \text{ }^\circ\text{K}$ and experiment appears quite satisfactory; in particular the minimum at temperatures close to $T = 0.37 \text{ }^\circ\text{K}$ is well verified. On the other hand, the melting curve obtained with Pomeranchuk's $T_C = 10^{-7} \text{ }^\circ\text{K}$, while also possessing a minimum close to $0.37 \text{ }^\circ\text{K}$, lies considerably above the experimental points for $T \cong 0.1 \text{ }^\circ\text{K}$. Experiments at even lower temperatures ($0.05 \text{ }^\circ\text{K} \leq T \leq 0.1 \text{ }^\circ\text{K}$) would be of great interest since a further distinction between our theory and Pomeranchuk's may be obtained by the observation or otherwise of the maximum in the melting curve at $T \cong 0.08 \text{ }^\circ\text{K}$ where our $\{S_{\text{sol}}(T, p, 0)\}_{\text{melt}}$ again equals $\{S_{\text{liq}}(T, p, 0)\}_{\text{melt}}$. In fact, granting the correctness of our $S_{\text{sol}}(T, p, 0)$, the absence of such a maximum would imply that the linear-in- T extrapolation of $S_{\text{liq}}(T, p, 0)$ for values of $T < 0.1 \text{ }^\circ\text{K}$ ²³ is incorrect and that the actual $S_{\text{liq}}(T, p, 0)$ has such an anomaly for $T < 0.1 \text{ }^\circ\text{K}$ (due for example to the onset of superfluidity) that our $\{S_{\text{sol}}(T, p, 0)\}_{\text{melt}}$ curve does not cross the actual $\{S_{\text{liq}}(T, p, 0)\}_{\text{melt}}$ curve for any $T < 0.1 \text{ }^\circ\text{K}$.

In concluding this section, we wish to emphasize that all the above results hold exactly only at zero external magnetic field. In the presence of such a magnetic field, B , we have from thermodynamics:

$$\frac{\partial G(T, p, B)}{\partial T} = -S(T, p, B), \quad \frac{\partial G(T, p, B)}{\partial p} = V(T, p, B), \quad (58)$$

$$\frac{\partial G(T, p, B)}{\partial B} = -M(T, p, B); \quad G \equiv F + pV - MB,$$

$$\{\Delta G(T, p, B)\}_{\text{melt}} \equiv \{G_{\text{liq}}(T, p, B)\}_{\text{melt}} - \{G_{\text{sol}}(T, p, B)\}_{\text{melt}} = 0. \quad (59)$$

Equations (58), (59) yield

$$\left\{ \frac{\partial p(T, B)}{\partial B} \right\}_{\text{melt}} = \frac{\{\Delta M(T, p, B)\}_{\text{melt}}}{\{\Delta V(T, p, B)\}_{\text{melt}}} \cong \frac{[\{x_{\text{liq}}(T, p, 0)\}_{\text{melt}} - \{x_{\text{sol}}(T, p, 0)\}_{\text{melt}}]B}{\{\Delta V(T, p, 0)\}_{\text{melt}}}, \quad (60)$$

$$\begin{aligned} \left\{ \frac{\partial p(T, B)}{\partial T} \right\}_{\text{melt}} &= \frac{\{\Delta S(T, p, B)\}_{\text{melt}}}{\{\Delta V(T, p, B)\}_{\text{melt}}} \cong \frac{\{\Delta S(T, p, 0)\}_{\text{melt}}}{\{\Delta V(T, p, 0)\}_{\text{melt}}} + \frac{\{(\partial/\partial B)\Delta S(T, p, B)\}_{B=0} B}{\{\Delta V(T, p, 0)\}_{\text{melt}}} \\ &= \frac{\{\Delta S(T, p, 0)\}_{\text{melt}}}{\{\Delta V(T, p, 0)\}_{\text{melt}}} + \frac{\{(\partial/\partial T)\Delta M(T, p, B)\}_{B=0} B}{\{\Delta V(T, p, 0)\}_{\text{melt}}} \\ &= \frac{\{\Delta S(T, p, 0)\}_{\text{melt}}}{\{\Delta V(T, p, 0)\}_{\text{melt}}} + \frac{[\{\partial x_{\text{liq}}(T, p, 0)/\partial T\}_{\text{melt}} - \{\partial x_{\text{sol}}(T, p, 0)/\partial T\}_{\text{melt}}]B^2}{\{\Delta V(T, p, 0)\}_{\text{melt}}}, \end{aligned} \quad (61)$$

and since

$$\{x_{\text{liq}}(T, p, 0)\}_{\text{melt}} < \{x_{\text{sol}}(T, p, 0)\}_{\text{melt}}, \quad \left\{ \frac{\partial x_{\text{liq}}(T, p, 0)}{\partial T} \right\}_{\text{melt}} > \left\{ \frac{\partial x_{\text{sol}}(T, p, 0)}{\partial T} \right\}_{\text{melt}}, \quad \{\Delta V(T, p, 0)\}_{\text{melt}} > 0,^{17}$$

²⁴ J. L. Baum, D. F. Brewer, J. G. Daunt, and D. O. Edwards, Phys. Rev. Letters 3, 127 (1959).

(see Fig. 1) we see that the field B decreases the value of p_{melt} at fixed T_{melt} and decreases the value of the temperature $T_0(B)$ [$T_0(0) \equiv T_0$] corresponding to the minimum of the melting curve.

To estimate the numerical magnitude of the effects involved, we integrate Eqs. (60), (61) and obtain

$$\frac{\{p(T_0, B)\}_{\text{melt}} - \{p(T_0, 0)\}_{\text{melt}}}{\{p(T_0, 0)\}_{\text{melt}}} \equiv \frac{\{p(T_0, B)\}_{\text{melt}} - p_0}{p_0} \approx -\frac{1}{2} \left(\frac{\mu B}{T_0} \right)^2 \left(\frac{\{T_{C; \text{liq}}\}_{\text{melt}} - \{T_{C; \text{sol}}\}_{\text{melt}}}{T_0} \right) \left(\frac{NT_0}{p_0 \Delta V(T_0, p_0, 0)} \right) \approx -\{0.5 \times 10^{-14} \text{ gauss}^{-2}\} B^2, \quad (62)$$

$$\frac{T_0 - T_0(B)}{T_0} \approx \frac{2}{0.2} \left(\frac{\mu B}{T_0} \right)^2 \left(\frac{\{T_{C; \text{liq}}\}_{\text{melt}} - \{T_{C; \text{sol}}\}_{\text{melt}}}{T_0} \right) \approx \{10^{-13} \text{ gauss}^{-2}\} B^2, \quad (63)$$

so that, for example, a field of 10^6 gauss is required to shift the melting curve minimum from $T_0 = 0.37^\circ \text{K}$ to $T_0(B) = 0.33^\circ \text{K}$.

10. CONCLUSIONS

In this section we summarize the results we have obtained for solid He³ and compare them with experiment.

For solid He³ at low pressures, $p \approx 30$ atm, and low temperatures, $T \lesssim 1^\circ \text{K}$, we find:

(1) For an empirical nearest neighbor distance $R = 3.8 \text{ \AA}$,⁸ our calculation gives a value of $0.36R$ for the root mean square deviation, δ , of an atom from its lattice site. The experimental value of δ for solid He³ is not known but it should be somewhat larger than the corresponding value for solid He⁴ which is known experimentally to be $0.31R$.¹⁰

(2) The cohesive energy per He³ atom in the solid at zero pressure is found to be roughly 2.4°K . Again

there is no experimental data available for solid He³ but its cohesive energy should be only a little less than the corresponding value for liquid He³ which is approximately 2.5°K .¹⁶

(3) From the algebraic sign and numerical value of the "exchange integral" J we predict that solid He³ should be a nuclear antiferromagnetic at $p \approx 30$ atm with a "paramagnetic" Curie temperature $T_C \approx 0.1^\circ \text{K}$. Nuclear magnetic resonance experiments⁶ indicate that solid He³ is indeed antiferromagnetic with $T_C \approx 0.1^\circ \text{K}$. We further predict that T_C decreases with increasing pressure and may even change sign at $p \approx 150$ atm; we may thus, very tentatively, anticipate a nuclear antiferromagnetic to nuclear ferromagnetic transition in solid He³ at such pressures and sufficiently low temperatures ($T \lesssim 0.1^\circ \text{K}$).

(4) We predict that the specific heat of solid He³ should exhibit a singularity at $T \approx 0.1^\circ \text{K}$ associated with the alignment of the nuclear spins. Only preliminary experimental data are available.²¹

(5) We also predict that the thermal expansion coefficient of solid He³ should become negative below about 0.6°K . Again no experimental data are available for solid He³, but experiments of Brewer and Daunt²³ have demonstrated a similar effect in liquid He³. *Note added in proof.*—S. G. Sydorak, R. L. Mills, and E. R. Grilly [Phys. Rev. Letters 4, 495 (1960)] report experimental data indicating that the thermal expansion coefficient of solid He³ becomes negative along the melting curve for $T_{\text{melt}} \lesssim 1^\circ \text{K}$.

(6) From (5) it follows that below $\approx 0.6^\circ \text{K}$ an isentropic compression (expansion) of solid He³ should produce a cooling (heating) effect [1% decrease (increase) in T per atm for $T \ll T_C$]. Fairbank and Walters⁶ have observed such an effect below about 0.4°K but their results are not conclusive since they allowed the solid to melt during the isentropic expansion.

(7) Finally, we construct the melting curve of He³ (p_{melt} vs T_{melt}) for $T < 0.5^\circ \text{K}$ and predict a minimum

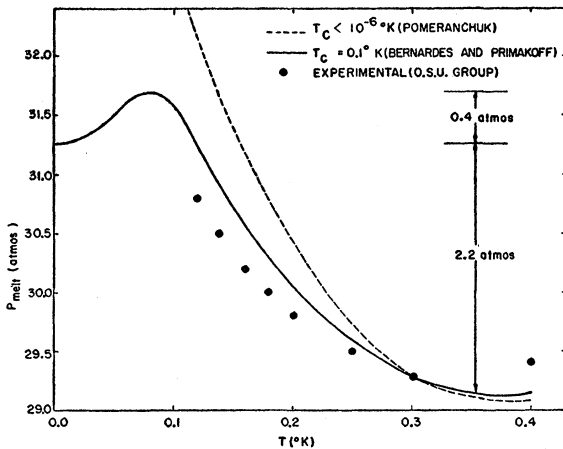


FIG. 5. Melting curves of He³, calculated from Eq. (57) and Fig. 4, for $T_C = 0.1^\circ \text{K}$ and $T_C < 10^{-6}^\circ \text{K}$; the dots represent experimental points (reference 24).

in this curve at $T \approx 0.37^\circ\text{K}$ and a maximum at $T \approx 0.08^\circ\text{K}$. The predicted minimum has recently been found (at $T = 0.32^\circ\text{K}$) in the experiment of Baum, Brewer, Daunt, and Edwards.²⁴ *Note added in proof.*—See in addition S. G. Sydoriak, R. L. Mills, and E. R. Grilly, Phys. Rev. Letters 4, 495 (1960), and D. M. Lee, H. A.

Fairbank, and E. J. Walker, Bull. Am. Phys. Soc. 4, 239 (1959), whose experiments show this minimum at 0.330°K and 0.32°K , respectively. We also consider the influence of an external magnetic field on the melting curve and find that very high fields ($\approx 10^6$ gauss) are required for an appreciable effect.

Lattice Dynamics of Alkali Halide Crystals*

A. D. B. WOODS, W. COCHRAN,[†] AND B. N. BROCKHOUSE
Physics Division, Atomic Energy of Canada Limited, Chalk River, Ontario, Canada
 (Received March 11, 1960)

The paper comprises theoretical and experimental studies of the lattice dynamics of alkali halides. A theory of the lattice dynamics of ionic crystals is given based on replacement of a polarizable ion by a model in which a rigid shell of electrons (taken to have zero mass) can move with respect to the massive ionic core. The dipolar approximation then makes the model exactly equivalent to a Born-von Kármán crystal in which there are two "atoms" of differing charge at each lattice point, one of the "atoms" having zero mass. The model has been specialized to the case of an alkali halide in which only one atom is polarizable, and computations of dispersion curves have been carried out for sodium iodide. We have determined the dispersion $\nu(\mathbf{q})$ relation of the lattice vibrations in the symmetric [001], [110], and [111] directions of sodium iodide at 110°K by the methods of neutron spectrometry.

The transverse acoustic, longitudinal acoustic, and transverse optic branches were determined completely with a probable error of about 3%. The dispersion relation for the longitudinal optic (LO) branch was determined for the [001] directions with less accuracy. Frequencies of some important phonons with their errors (units 10^{12} cps) are: TA[0,0,1] 1.22 ± 0.04 , LA[0,0,1] 1.82 ± 0.06 , TA[$\frac{1}{2}, \frac{1}{2}, \frac{1}{2}$] 1.52 ± 0.05 , LA[$\frac{1}{2}, \frac{1}{2}, \frac{1}{2}$] 2.32 ± 0.06 , TO[0,0,0] 3.60 ± 0.1 , TO[0,0,1] 3.80 ± 0.1 , TO[$\frac{1}{2}, \frac{1}{2}, \frac{1}{2}$] 3.50 ± 0.1 . The agreement between the experimental results and the calculations based on the shell model, while not complete, is quite satisfactory. The neutron groups corresponding to phonons of the LO branch were anomalously energy broadened, especially for phonons of long wavelength, suggesting a remarkably short lifetime for the phonons of this branch.

1. INTRODUCTION

THE lattice dynamics of a crystal is described by a frequency, wave vector dispersion relation, insofar as it is harmonic. In the last few years it has become possible to determine experimentally this dispersion relation using x-ray diffraction and neutron spectrometry. The dispersion relation has been measured fairly accurately for several metallic¹⁻⁴ and semiconducting⁵⁻⁷ crystals consisting of one kind of atom. The only determinations for crystals having more than one kind of atom^{8,9} have been by x-ray diffraction methods. However, there is good reason to believe that neutron

measurements are much more accurate than are x-ray measurements for crystals with more than one atom per unit cell. Thus it seems desirable to study such crystals by neutron spectrometry.

In the determination of the dispersion relation by neutron spectrometry energy distributions of initially monoenergetic neutrons are measured after scattering by a single crystal in known orientation. The frequencies ν and wave vectors \mathbf{q} of the vibrations are inferred from conservation of energy and momentum between the neutrons and single phonons.^{3,10,11} If the frequencies and wave vectors of the phonons are well defined, then sharp groups (broadened of course by imperfect resolution) are observed in the neutron energy distributions. The center of a neutron group is taken to define the energy (E') and wave vector (\mathbf{k}') of those neutrons which had interacted with a particular vibration. The frequency and wave vector of the vibration are given by the conservation equations

$$\begin{aligned} E_0 - E' &= \pm \hbar \nu \equiv \pm \hbar \omega, \\ \mathbf{Q} \equiv \mathbf{k}_0 - \mathbf{k}' &= 2\pi \boldsymbol{\tau} - \mathbf{q}, \end{aligned} \quad (1.1.1)$$

where E_0 and \mathbf{k}_0 are the energy and momentum of the incident neutrons, and $\boldsymbol{\tau}$ is any vector of the reciprocal

* This paper was presented at the Washington, D. C., Meeting of the American Physical Society, April 30–May 2, 1959 [Bull. Am. Phys. Soc. 4, 246 (1959)].

[†] Visiting scientist from the Cavendish Laboratory, Cambridge, England, now returned.

¹ E. H. Jacobsen, Phys. Rev. 97, 654 (1955). Earlier references to x-ray work are given here.

² C. B. Walker, Phys. Rev. 103, 547 (1956).

³ B. N. Brockhouse and A. T. Stewart, Revs. Modern Phys. 30, 236 (1958). Earlier references to neutron work are given here.

⁴ B. N. Brockhouse, T. Arase, G. Caglioti, M. Sakamoto, R. N. Sinclair, and A. D. B. Woods, Bull. Am. Phys. Soc. 5, 39 (1960).

⁵ B. N. Brockhouse and P. K. Iyengar, Phys. Rev. 111, 747 (1958).

⁶ A. Ghose, H. Palevsky, D. J. Hughes, I. Pelah, and C. M. Eisenhauer, Phys. Rev. 113, 49 (1959).

⁷ B. N. Brockhouse, Phys. Rev. Letters 2, 256 (1959).

⁸ H. Cole, J. Appl. Phys. 24, 482 (1953).

⁹ D. Cribier, Ann. phys. 4, 333 (1959).

¹⁰ R. Weinstock, Phys. Rev. 65, 1 (1944).

¹¹ G. Placzek and L. Van Hove, Phys. Rev. 93, 1207 (1954).